Structural and optical properties of InGaN/GaN nanowire heterostructures grown by PA-MBE

2011 Nanotechnology 22 075601

(http://iopscience.iop.org/0957-4484/22/7/075601)

Nanotechnology **22** (2011) 075601 (8pp) doi:10.1088/0957-4484/22/7/075601

Structural and optical properties of InGaN/GaN nanowire heterostructures grown by PA-MBE

G Tourbot[1,2,4], C Bougerol[3], A Grenier[1], M Den Hertog[3], D Sam-Giao[2], D Cooper[1], P Gilet[1], B Gayral[2] and B Daudin[2]

[1] CEA, LETI, MINATEC, 38054 Grenoble, France
[2] CEA-CNRS-UJF group 'Nanophysique et Semiconducteurs', CEA, INAC, SP2M, NPSC, 17 rue des Martyrs, 38 054 Grenoble, France
[3] CEA-CNRS-UJF group 'Nanophysique et Semiconducteurs', Institut Néel/CNRS, 25 rue des Martyrs, 38 042 Grenoble, France

E-mail: gabriel.tourbot@cea.fr

Received 16 September 2010, in final form 23 November 2010
Published 14 January 2011
Online at stacks.iop.org/Nano/22/075601

Abstract
The structural and optical properties of InGaN/GaN nanowire heterostructures grown by plasma-assisted molecular beam epitaxy have been studied using a combination of transmission electron microscopy, electron tomography and photoluminescence spectroscopy. It is found that, depending on In content, the strain relaxation of InGaN may be elastic or plastic. Elastic relaxation results in a pronounced radial In content gradient. Plastic relaxation is associated with the formation of misfit dislocations at the InGaN/GaN interface or with cracks in the InGaN nanowire section. In all cases, a GaN shell was formed around the InGaN core, which is assigned to differences in In and Ga diffusion mean free paths.

(Some figures in this article are in colour only in the electronic version)

1. Introduction

For practical applications as well as for more basic studies, III-nitride nanowires (NWs) are an attractive option to overcome difficulties arising from the high density of crystallographic defects encountered in two-dimensional (2D) layers of GaN, AlN and InN. These defects consist of threading edge dislocations, screw dislocations and mixed dislocations, most of them originating from the coalescence of growing grains. By contrast, NWs, which can be viewed as an ensemble of vertically elongated non-coalesced grains, consist of high quality material which is free of dislocations and exhibits excellent optical properties [1–4].

As a further option to improve optical properties, zero-dimensional quantum objects ('quantum dots') have proved to be an efficient way of confining carriers, leading to a suppression of non-radiative recombination up to room temperature [5]. The bottom-up formation of such structures is often achieved using the so-called Stranski–Krastanow 2D–3D transition which is driven by the lattice mismatch between the substrate and the deposited layer. In contrast, axial heterostructures in nanowires behave like quantum dots [4, 6] and do not require any lattice mismatch to be grown.

Moreover, it has been theoretically predicted that, depending on their diameter, NW geometry might drastically increase the critical thickness of non-lattice-matched heterostructures [7, 8]. This peculiarity provides an additional advantage for growing InGaN/GaN or AlGaN/GaN NW heterostructures with a high concentration of In or Al, eventually making it possible to extend the wavelength range of light emitting diodes (LEDs) into the green or the UV. Indeed, based on the above considerations, the realization of NW LEDs in the visible [9–12] and in the UV [13] wavelength range has been demonstrated.

However, despite these promising achievements, the growth of InGaN/GaN NW heterostructures remains largely unexplored. On the one hand, it has been theoretically predicted that both strain relaxation and light emission

[4] Author to whom any correspondence should be addressed.

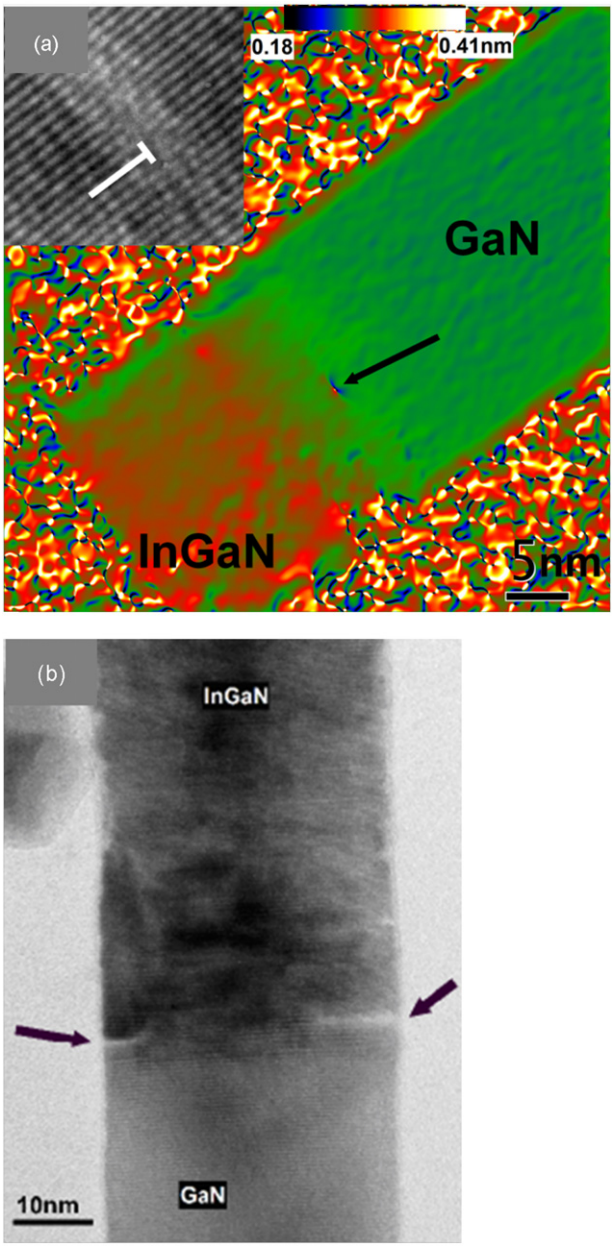

Figure 1. (a) Geometrical phase analysis of a nanowire of high nominal In composition (43%) showing a misfit dislocation at the InGaN/GaN interface (in the inset, a zoom on the original HRTEM image is shown; interfringe spacing: 0.276 nm). (b) HRTEM of a nanowire exhibiting cracks in the walls.

tunability range of InGaN NWs should be favored with respect to 2D layers [14], consistent with the experimental findings of Kuykendall *et al* who have grown $In_xGa_{1-x}N$ NWs for x ranging from 0 to 1 by low-temperature halide chemical vapor deposition [15]. On the other hand, clustering in InGaN/GaN NW heterostructures has been recently reported [16], emphasizing the influence of strain relaxation mechanisms on both structural and optical properties of such heterostructures.

It is the aim of the present work to address the strain relaxation issue of InGaN/GaN NW heterostructures grown by plasma-assisted molecular beam epitaxy (PA-MBE). It will be shown that, depending on In content, strain relaxation of an InGaN section on GaN NW may occur either elastically or plastically. Elastic strain relaxation has been found to be associated with In-rich cluster formation. Plastic relaxation has been found to result from interfacial dislocation formation or from cracks in the (0001) basal plane at the interface between GaN and InGaN. In all cases, the formation of self-organized InGaN/GaN core/shell structures has also been put in evidence. This behavior provides new insights on the light emission variability of GaN/InGaN/GaN NW LEDs grown on non-patterned substrates [11, 17], suggesting that it could be partly due to In concentration fluctuations correlated to the randomness of spontaneous NW nucleation.

2. Experimental details

2.1. Samples

InGaN/GaN nanowires were grown on (111) Si by plasma-assisted molecular beam epitaxy (PA-MBE). Prior to introduction in the growth chamber, the 2 inch substrate was de-oxidized for 40 s in (10%) HF. Next it was mounted In-free on a sample holder and outgassed at high temperature until the appearance on the reflection high-energy electron diffraction (RHEED) pattern of a clear 7×7 reconstruction, characteristic of a clean (111) Si surface. Before each experiment, the growth temperature was measured in a reproducible way by exposing the bare Si surface to Ga flux and measuring Ga desorption time by RHEED [18].

A thin (2–3 nm) AlN buffer layer was used in order to improve wire twist [19] and tilt [20]. Next, a 300 nm GaN base was grown in the standard N-rich, high-temperature conditions: the III/V ratio was fixed to 0.25, and the substrate temperature was in the 850 °C range. The substrate temperature was then lowered to 590 °C to allow the growth of InGaN [21], which was deposited on top of the GaN nanowire base in highly N-rich conditions, i.e. an $(In + Ga)/N$ ratio of about 1/6. The In nominal composition was defined as the $In/(In + Ga)$ flux ratio value. The samples were rotated during growth to avoid shadowing effects and promote a homogeneous growth. This resulted in well-oriented NWs with diameters ranging from 20 to 40 nm.

2.2. High resolution electron microscopy analysis

Nanowires (NWs) with different nominal In compositions ranging from 15% to 60% were scraped off the substrate and dispersed on a Cu microscope grid covered with a holey carbon film. They were investigated by high resolution transmission electron microscopy (HRTEM) performed on a Jeol 4000EX microscope operated at 400 kV ($Cs = 1$ mm) coupled with geometrical phase analysis (GPA) [22] in order to obtain maps of the a and c interplanar spacings. The reference region was always taken in the GaN part of the InGaN/GaN NW heterostructure.

For high nominal In composition, typically above 40%, the HRTEM images show that the NWs present a flat top surface. Furthermore, two types of defects have been observed (figure 1). They consist of either cracks appearing on the lateral sides of the NWs (figure 1(b)) or

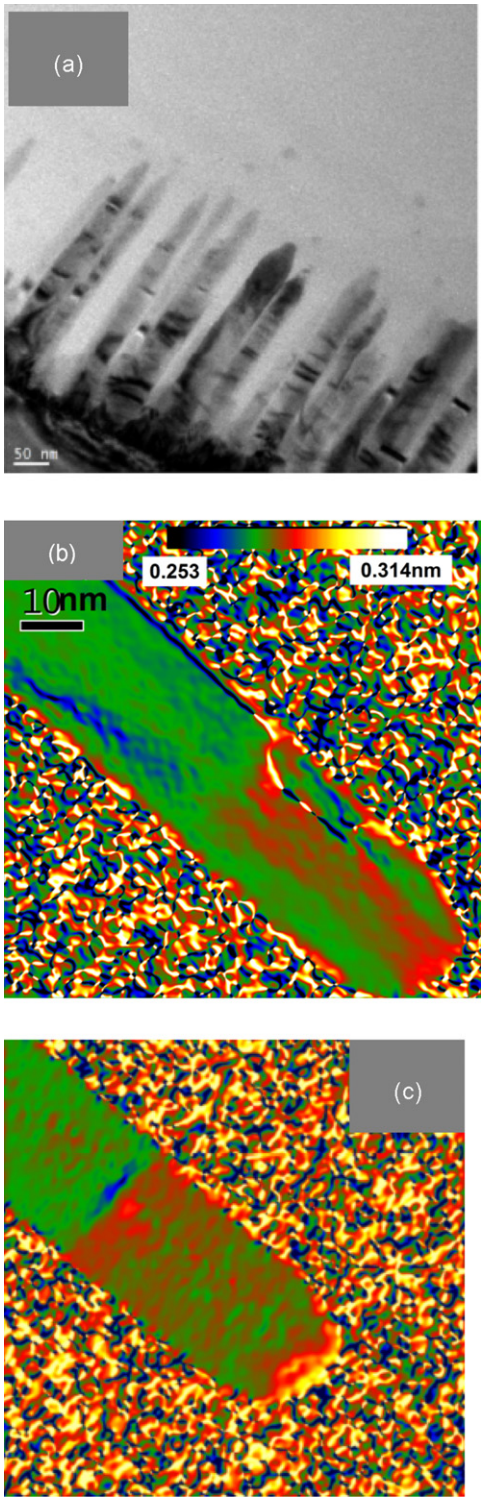

Figure 2. (a) TEM micrograph of an assembly of nanowires with a low nominal In composition (17%) and single-wire GPA cartographies of (b) *a*-spacing and (c) *c*-spacing.

misfit dislocations at the InGaN/GaN interface (figure 1(a)) characterized by the insertion of an extra $(10\bar{1}0)$ plane seen in the inset of figure 1(a). These edge-type dislocations of Burgers vector $b = 1/3\langle\bar{1}2\bar{1}0\rangle$, typical of nitride heterostructures, have already been reported in the case of AlN/GaN heterostructures [23].

These structural defects, namely cracks and misfit dislocations, are the signatures of two different plastic strain relaxation mechanisms which allow for the accommodation of the large lattice mismatch in this composition range. The *a*-spacing map given in figure 1(a) shows that this lattice parameter is uniform over the whole InGaN region, except for a small shell on the lateral sides. Even though the lattice parameters alone cannot lead to the In content determination, since they are also affected by the strain state, this observation indicates that no In clustering occurs in these nanowires.

By contrast, for low nominal In composition, up to ∼25%, the NWs present a pencil-like shape (figure 2(a)). The cartography of the *a*-spacing given in figure 2(b) clearly shows that this parameter is not uniform in the InGaN part as in the previous case but presents a core–shell-like distribution [24]. The shell, about 6 nm thick, has the same *a* parameter as the GaN base of the nanowire, whereas the core part has a larger one. The colored *c*-map (figure 2(c)) does not show the core–shell-like distribution but reveals some inhomogeneities. This situation is very comparable to what we have observed in GaN nanowires covered with an AlN shell [24], i.e. an almost full relaxation of both AlN and GaN in the *a*-direction and a common *c*-parameter. These observations seem therefore to indicate that, for low nominal In composition, a spontaneous core–shell structure is formed in relation with In clustering, whereas the defects present at high-In content allow the formation of homogeneous InGaN material.

2.3. Energy-dispersive x-ray spectroscopy analysis

The GPA is insufficient to determine the In content in the InGaN section since, as mentioned above, the lattice parameters also depend on the strain state. In order to overcome this intrinsic limitation of the GPA, the same samples have also been studied by energy-dispersive x-ray spectroscopy (EDX) on a field-emission scanning microscope (Hitachi 5500) operated at 30 kV. It should be mentioned that the quantification has been made without standards, which implies that the analysis is not fully quantitative. Figures 3(b) and (c) show the In axial and transverse concentration profiles obtained on a high nominal In composition nanowire. Along the growth direction, the In content remains constant and equal to 56%, whereas the transverse line-scan reveals an In-poor layer extending roughly over 3 nm all around the InGaN part of the NW. In the case of low nominal In composition, axial line-scans show fluctuations in the In content (figure 4(b)), consistent with the presence of In-rich clusters. On transverse line-scans (figure 4(c)), we observe that only the core of the nanowire contains In, which confirms the spontaneous formation of the core–shell structure previously deduced from HRTEM experiments.

2.4. Electron tomography analysis

HRTEM or EDX can only give two-dimensional information integrated along the projection direction. Therefore, to obtain reliable 3D morphological and chemical information, electron tomography was performed in high-angle annular dark field scanning transmission electron microscopy mode using a

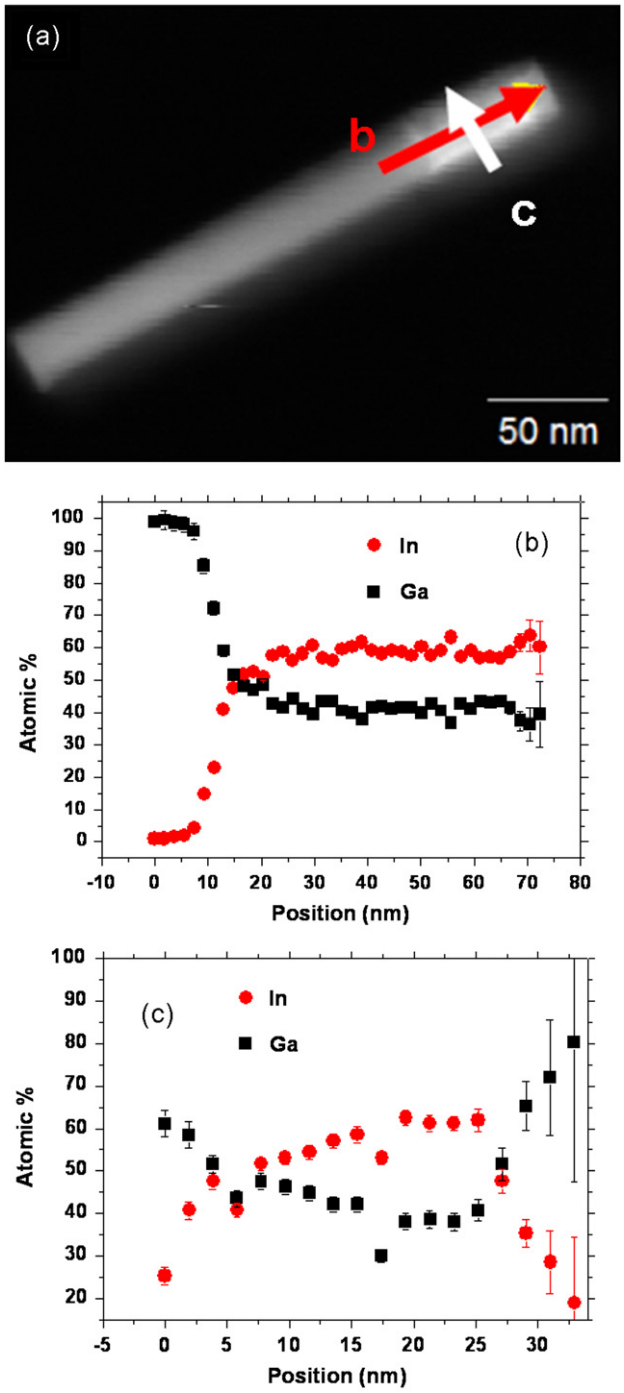

Figure 3. (a) STEM micrograph of a single InGaN/GaN nanowire with a high nominal In composition, (b) axial and (c) transverse EDX line-scans. Position zero corresponds to the arrow starting point.

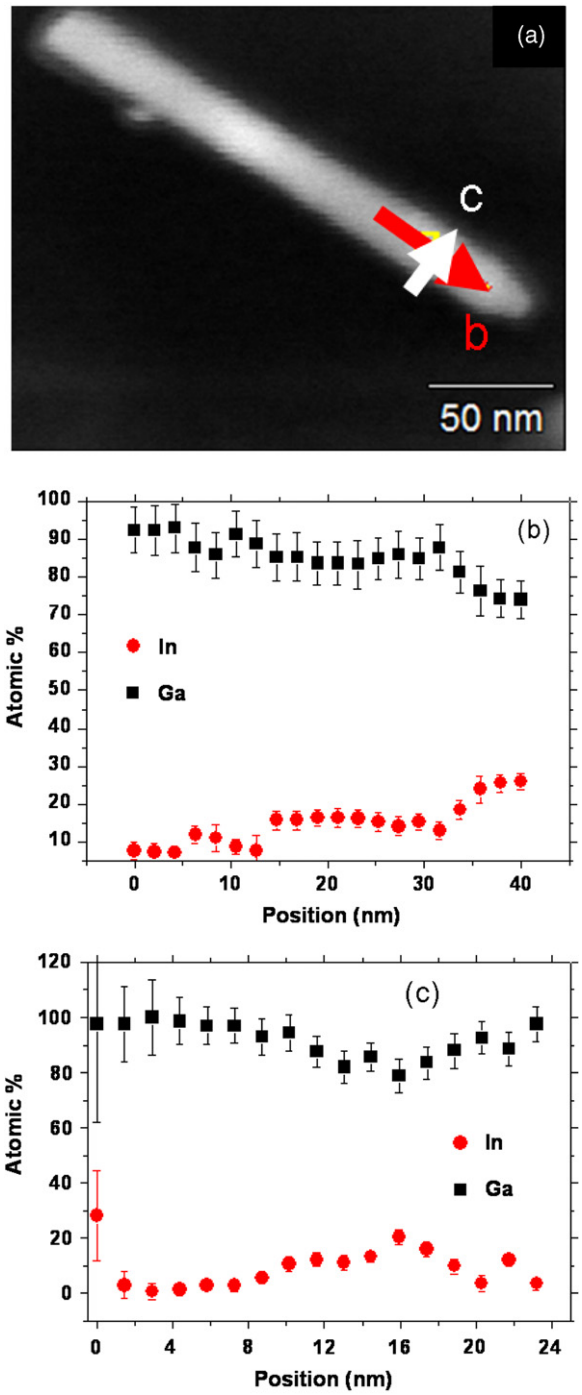

Figure 4. (a) STEM micrograph of a single InGaN/GaN nanowire with a low nominal In composition, (b) axial and (c) transverse EDX line-scans. Position zero corresponds to the arrow starting point.

TITAN FEI TEM microscope at 200 kV equipped with a 2020 Fischione tomography holder. The convergence angle used was 7.5 mrad in order to obtain a depth of focus better than 50 nm, allowing focus on the whole nanowire at once [25]. The contrast is monotonic with thickness and is proportional to $Z^{1.8}$ (where Z is the atomic number). The tilt series have been acquired between $\pm 75°$, with 2° increment, allowing one to avoid contamination of the sample, and resulting in 76 images. According to the missing wedge artifact due to the incomplete tilt range of the holder, resolutions along and perpendicular to the nanowire axis are estimated to be around 3 nm and 5 nm, respectively.

Post-alignment of images and reconstructions using an iterative reconstruction algorithm were carried out with the FEI Inspect 3D software. Amira and Chimera software were used for the 3D visualization of the reconstructed volume, using the isosurface in order to separate the GaN and InGaN phases. The threshold for the isosurface has been set up from intensities corresponding to GaN and InGaN phases.

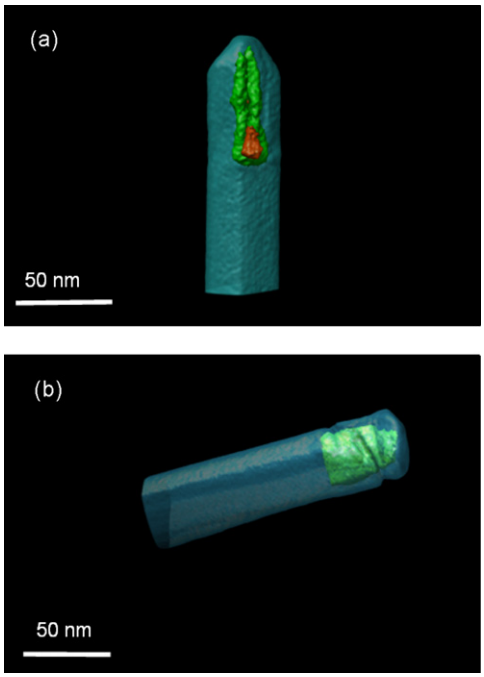

Figure 5. Electron tomographies of single InGaN/GaN nanowires ((a) nominally low and (b) nominally high-In content); the isosurface reconstruction shows the In-enriched cores.

Figures 5(a) and (b) show an isosurface representation of the tomogram acquired from single nanowires originating from nominally In-poor and In-rich samples, respectively. The overall shape of the nanowires (pencil-like and flat top, respectively) is well confirmed, as well as the spontaneous formation of a core–shell structure. The InGaN core diameters were estimated to be 20 nm and 29 nm, for nominally low- and high-In compositions, respectively, while the total diameter is about 40 nm. In the former, the In distribution is inhomogeneous, as evidenced by the presence, close to the InGaN/GaN interface, of an In-rich cluster (orange in figure 5(a)), about 10 nm in average diameter, surrounded by an In-poor InGaN (green) core and an outer shell of pure GaN (blue).

2.5. Photoluminescence spectroscopy

Photoluminescence experiments on as-grown nanowire ensembles were conducted from 7 to 300 K in a cold finger cryostat. The samples were photoexcited with a frequency-doubled continuous wave Ar laser (244 nm), the excitation power being controlled from 0.8 to 40 W cm^{-2}.

Figure 6 shows the temperature-dependent photoluminescence spectra of two representative samples grown with nominal In concentrations of 11% (figure 6(a)) and 43% (figure 6(b)), hereafter denoted sample (a) and (b) respectively. Interestingly, sample (a) exhibits an intense 7 K luminescence peak centered at 2.24 eV, corresponding to an In content far greater than the nominal (i.e. based on the In/(In + Ga) flux ratio) one. This confirms that, in spite of the local alloy inhomogeneities, the local potential variations do not prevent the carriers from diffusing and relaxing to the In-rich core of

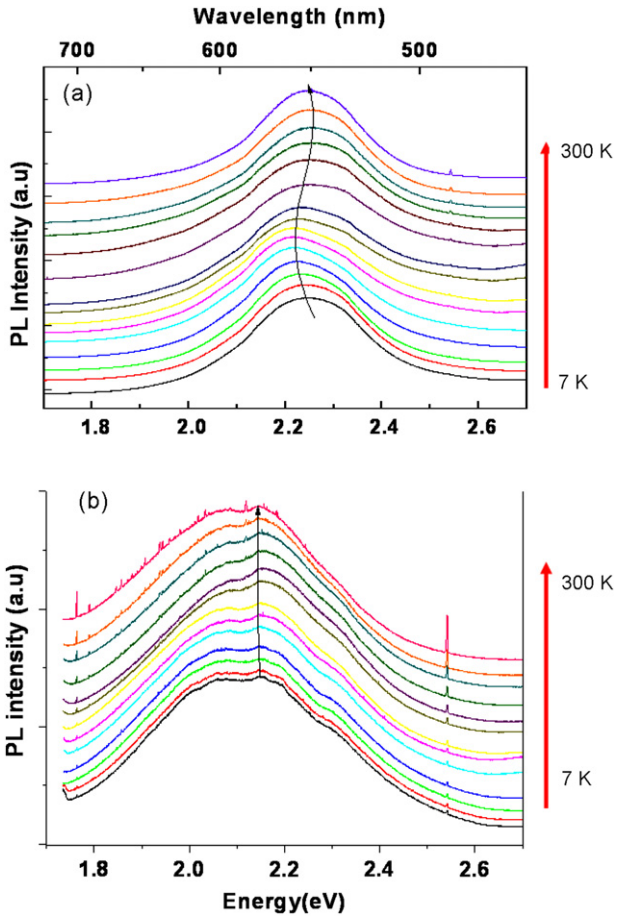

Figure 6. Temperature-dependent PL spectra of samples with a nominal In content of (a) 11% and (b) 43%.

the nanowire. Indeed, luminescence stemming from low-In content InGaN is negligible as the PL intensity above 2.6 eV is much smaller than the main luminescence peak, although structural studies show that a large part of the nanowire contains a low-In content. In other words the rather narrow luminescence peak (full width at half maximum ∼250 meV) does not reflect the broad distribution of In content (ranging approximately from 0 to 40%) in the InGaN nanowire. In contrast, the emission of sample (b) fits rather well the nominal In content if we assume a bandgap variation of

$$E_g = 3.51(1-x) + 0.69x - 1.4x(1-x) \qquad (1)$$

where E_g is the alloy bandgap at 7 K and x the In/(In + Ga) ratio [26, 27].

Sample (a) exhibits a marked S-shaped shift of the peak position with temperature [28], associated with localization–delocalization of excitons trapped in the band-tail states [29, 30]. This hypothesis is further supported by the results of figure 7, which depicts the peak position of sample (a) as a function of the temperature at different excitation power densities. One can see that an increase of the excitation power leads to a disappearance of this 'S-shaped' variation: by saturating the local potential minima, one recovers the expected bandgap temperature dependence as

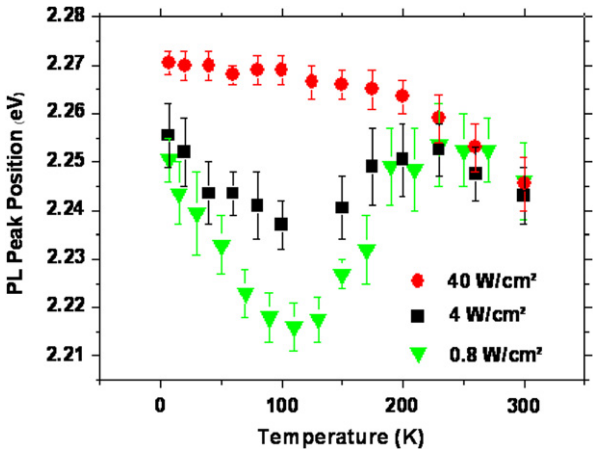

Figure 7. PL spectral peak position in sample (a), at different values of excitation power density.

fitted by the Varshni law:

$$E_g(T)\colon E_g(0\ \mathrm{K}) - \frac{\alpha T^2}{\beta + T} \qquad (2)$$

with $E_g(0\ \mathrm{K}) = 2.271$ eV, $\alpha = 0.001$ eV K^{-1}. and $\beta = 3950$ K. These values show a temperature behavior comparable with that of 2D layers [31].

In contrast, the comparison of figures 6(a) and (b) shows that no exciton delocalization could be observed in sample (b), as emission does not shift when the temperature increases, even at low excitation power. These exciton delocalization effects will be discussed in more detail in section 3.

3. Discussion

The above results have put in evidence that elastically strained InGaN NWs deposited on a GaN basis may relax either plastically or elastically, depending on In content, i.e. on the in-plane lattice mismatch at the InGaN/GaN interface. The issue of plastic strain relaxation of III-nitride NW heterostructures has been theoretically addressed by Ertekin *et al*, using an approach based on the Matthews model extended to the NW geometry [7]. Considering that the Burgers vector of the misfit dislocation at the InGaN/GaN interface is of the 1/3 [11–20] type, with a modulus equal to $a \sim 0.3$ nm, it is expected that for NWs with a diameter of 40 nm and for an In content of 50% corresponding to a lattice mismatch of about 6%, plastic relaxation should occur, in agreement with our findings. By contrast, for In content in the 10–20% range, the situation is more complicated and it is found that plastic relaxation could occur or not depending on small variations of In content and on the value of the Burgers vector.

Remarkably, whatever the concentration of In in the InGaN NW section is, the formation of a pure GaN shell has been put in evidence. Such a spontaneous core–shell feature has already been reported in InGaN and AlGaN nanowires grown by chemical vapor deposition [32–34]. A similar behavior has also been observed in nanowires grown by MBE in the simpler GaN/AlN system: successive deposition of GaN and AlN on preexisting GaN nanowires led to the lateral growth of an AlN shell, attributed to the low surface mobility of Al adatoms, which are incorporated before reaching the nanowire top [35–37]. We suggest that, similarly, at the low temperature adapted to the growth of InGaN, the Ga adatom mobility is strongly reduced, resulting in sidewall incorporation. In the limit of no adatom diffusion and only considering geometrical effects, it has been predicted that the ratio v_L/v_V is equal to $\tan(\alpha)/\pi$, where v_L and v_V are the lateral and vertical growth rates, respectively, and α is the impinging angle of the metal flux with respect to the NW axis [38]. In our case where α is about 25°, it is found that the thin GaN shell in figure 1 should be about 1.5 nm thick, in excellent agreement with the TEM observations and consistent with the absence of Ga diffusion on the sidewalls of NWs when growing InGaN.

This simple mechanism accounts for a natural InGaN/GaN core–shell formation for both nominally low- and high-In compositions. Nevertheless, it does not account for the fact that the GaN shell was found to be significantly thicker in the case of low-In content samples, as put in evidence by HRTEM and electron tomography experiments. Another mechanism is therefore needed to account for the thicker shell of the InGaN/GaN core–shell structure spontaneously formed when growing InGaN with a low nominal In flux.

It is well known that alloying/segregation may be an efficient mechanism to relieve strain in heterostructures. As a matter of fact, alloying was found to occur in InAs/InP Stranski–Krastanow (SK) quantum dots, resulting in composition alteration of the dots associated with partial elastic strain relaxation [39]. More generally, it has been widely established that inhomogeneous strain relaxation occurring in 3D structures can lead to strong differences in local alloy composition within a single quantum dot [40, 41]. Additionally, the composition of thin alloy layers can be restrained to values limiting the strain energy caused by the mismatch with an underlying layer; this is the so-called lattice pulling effect [42, 43]. This effect is strain-dependent, tending to vanish for increasing layer thickness associated with decreasing strain state, eventually leading to an alloy composition identical to the expected nominal one.

In the case of low-In content InGaN NWs, the formation of a GaN shell thicker than in the case of high-In content material suggests that Ga/In adatom strain-induced segregation is occurring during growth. More precisely, in the absence of plastic strain relaxation, it is suggested that InGaN deposited on the top of GaN nanocolumns is relaxing elastically by adopting a pyramidal shape similar to that of an SK quantum dot [44]. Interestingly, such a pyramidal shape has been recently observed for InGaN insertions embedded in GaN nanowires [16]. It is then expected that the lattice parameter will be expanded at the top of the InGaN pyramid, as a result of elastic strain relaxation and also possibly from a vertical In gradient which could be assigned to the aforementioned lattice pulling effect. As a consequence, further incorporation of In in the alloy will be easier on the top of the InGaN pyramid than on the sides. Conversely, Ga incorporation is expected to be unfavorable on the top of the InGaN pyramid, while it

should be favorable at the base of it, which is matched to a relaxed GaN NW. Such a segregation-induced strain relaxation process should be self-maintained all along the growth of the InGaN section, leading to the spontaneous formation of an InGaN/GaN core/shell structure. This model is supported by the observation of a pencil-like shape of the InGaN section, whatever its length is. By contrast, in the case of samples grown with a higher nominal In content, plastic relaxation is found to occur very early during the deposition of InGaN, as shown by the HRTEM images (see figure 1). The resulting strain uniformity leads to homogeneous (on the scale of a few tens of nanometers) In and Ga incorporation in our structure and to a flat top of the NW. In the absence of a driving force for Ga and In segregation, the InGaN composition is then found to be homogeneous and consistent with the expected nominal value while GaN shell formation is limited to the one which results from low Ga diffusion at the low growth temperature of InGaN alloy.

Now turning towards the optical properties of InGaN NWs, it has been found that samples (a) and (b) exhibit a strong photoluminescence in the 2–2.2 eV range, as an evidence that excitons recombine in areas of similar In content. Nevertheless, their temperature variation proves that the local potential landscape is qualitatively different. In sample (a), the short-scale (typically around 1 nm) potential minima are shallow and near enough to allow delocalization and diffusion at reasonable temperatures, whereas the energy barriers to exciton diffusion are much higher in sample (b).

The photoluminescence properties of our samples are related to the local electronic properties of the materials: the exciton localization length was found to be about 2 nm in InGaN/GaN quantum wells [45], and their trapping length is considered to be about 4 nm [46]. The nature of the localizing centers in InGaN is not definitively established, either small-scale (a few nanometers) In-rich clusters [47, 48] or randomly formed In–N–In chains [49]. We tentatively suggest that there is an important local (1 nm scale) alloy disorder in the high-In content NWs resulting in deep potential minima. In that case, at any temperature in the 4–300 K range, photocreated carriers relax towards the neighboring quantum dot-like potential minimum and stay trapped until radiative recombination occurs (note that relaxation towards non-radiative centers can also occur). In contrast, samples grown with a low-In flux exhibit gross (10 nm scale) clustering, but inside a single cluster the alloy is comparatively more homogeneous, allowing for easy exciton delocalization and diffusion. Photocreated carriers will thus diffuse and relax towards the In-rich regions of the nanowire where they can then be trapped in short-scale localized states. At intermediate temperatures (7–100 K), detrapping and further relaxation to slightly deeper localized states can occur, while at higher temperatures thermal filling of shallow localized states is observed.

In conclusion, it has been demonstrated that depending on In content, strain relaxation of InGaN grown on GaN NWs may be elastic or plastic. Plastic strain relaxation has been observed in the case of In-rich InGaN and is associated with the formation of a relatively homogeneous alloy, with limited thermal delocalization of carriers. By contrast, In-poor alloy has been found to exhibit elastic strain relaxation, partly assigned to strain-induced Ga and In segregation. Depending on their thickness and In content, it is speculated that InGaN quantum wells embedded in GaN barriers should also exhibit the clustering effect. This emphasizes the need to accurately control the In content in view of practical applications, and furthermore suggests that in-plane ordered growth is a requirement to limit the In content variability from one NW to another.

Acknowledgments

This work was partly supported by the French National Research Agency (ANR) through Carnot founding and through Nanoscience and Nanotechnology Program (Project BONAFO No ANR-08-NANO-031-01).

References

[1] Ristic J, Calleja E, Sanchez-Garcıa M A, Ulloa J M, Sanchez-Paramo J, Calleja J M, Jahn U, Trampert A and Ploog K H 2003 *Phys. Rev.* B **68** 125305
[2] Schlager J B, Sanford N A, Bertness K A, Barker J M, Roshko A and Blanchard P T 2006 *Appl. Phys. Lett.* **88** 213106
[3] Yi S N *et al* 2007 *Appl. Phys. Lett.* **90** 101901
[4] Renard J, Songmuang R, Bougerol C, Daudin B and Gayral B 2008 *Nano Lett.* **8** 2092
[5] Renard J, Kandaswamy P K, Monroy E and Gayral B 2009 *Appl. Phys. Lett.* **95** 131309
[6] Renard J, Songmuang R, Tourbot G, Bougerol C, Daudin B and Gayral B 2009 *Phys. Rev.* B **80** 121305
[7] Ertekin E, Greaney P A, Chrzan D C and Sands T D 2005 *J. Appl. Phys.* **97** 114325
[8] Glas F 2006 *Phys. Rev.* B **74** 121302(R)
[9] Kikuchi A, Kawai M, Tada M and Kishino K 2004 *Japan. J. Appl. Phys.* **43** L1524
[10] Kim H M, Cho Y H, Lee H S, Kim S I, Ryu S R, Kim D Y, Kang T W and Chung K S 2004 *Nano. Lett.* **4** 1059
[11] Bavencove A L *et al* 2010 *Phys. Status Solidi* a **207** 1425
[12] Armitage R and Tsubaki K 2010 *Nanotechnology* **21** 195202
[13] Sekiguchi H, Kishino K and Kikuchi A 2008 *Electron. Lett.* **44** 151
[14] Xiang H J, Wei S H, Da Silva J L F and Li J 2008 *Phys. Rev.* B **78** 193301
[15] Kuykendall T, Ulrich P, Aloni S and Yang P 2007 *Nat. Mater.* **6** 951
[16] Chang Y L, Wang J L, Li F and Mi Z 2010 *Appl. Phys. Lett.* **96** 013106
[17] Kishino K, Kikuchi A, Sekiguchi H and Ishizawa S 2007 *Proc. SPIE* **6473** 64730T
[18] Landré O, Songmuang R, Renard J, Bellet-Amalric E, Renevier H and Daudin B 2008 *Appl. Phys. Lett.* **93** 183109
[19] Largeau L, Dheeraj D L, Tchernycheva M, Cirlin G E and Harmand J C 2008 *Nanotechnology* **19** 155704
[20] Songmuang R, Landré O and Daudin B 2007 *Appl. Phys. Lett.* **91** 251902
[21] Adelmann C, Langer R, Feuillet G and Daudin B 1999 *Appl. Phys. Lett.* **75** 3518
[22] Hÿtch M, Snoeck E and Kilaas R 1998 *Ultramicroscopy* **74** 131
[23] Bourret A, Adelmann C, Daudin B, Rouvière J L, Feuillet G and Mula G 2001 *Phys. Rev.* B **63** 245307

[24] Hestroffer K, Mata R, Camacho D, Leclere C, Tourbot G, Niquet Y M, Cros A, Bougerol C, Renevier H and Daudin B 2010 *Nanotechnology* **21** 415702
[25] Reiler L 1997 *Transmission Electron Microscopy, Physics of Image Formation and Microanalysis* 4th edn (New York: Springer)
[26] Wu J, Walukiewicz W, Shan W, Yu K M, Ager J W, Li S X, Haller E E, Lu H and Shaff W J 2003 *J. Appl. Phys.* **94** 4457
[27] Wu J, Walukiewicz W, Yu K M, Ager J W, Li S X, Haller E E, Lu H and Shaff W J 2002 *Appl. Phys. Lett.* **80** 4741
[28] Hong C C, Ahn H, Wu C Y and Gwo S 2009 *Opt. Express* **17** 17227
[29] Eliseev P G, Perlin P, Lee J and Osiński M 1997 *Appl. Phys. Lett.* **71** 569
[30] Cho Y H, Gainer G H, Fischer A J, Song J J, Keller S, Mishra U K and DenBaars S P 1998 *Appl. Phys. Lett.* **73** 1370
[31] Schenk H P D, Leroux M and de Mierry P 2000 *J. Appl. Phys.* **88** 1525
[32] Cai X M, Leung Y H, Cheung K Y, Tam K H, Djurisic A B, Xie M H, Chen H Y and Gwo S 2006 *Nanotechnology* **17** 2330
[33] Su J *et al* 2005 *Appl. Phys. Lett.* **87** 183 108
[34] Choi H, Johnson J C, He R, Lee S, Kim F, Pauzauskie P, Goldberger J, Saykally R J and Yang P 2003 *J. Phys. Chem. B* **107** 8721
[35] Ristic J, Calleja E, Trampert A, Fernandez-Garrido S, Rivera C, Jahn U and Ploog K H 2005 *Phys. Rev. Lett.* **94** 146102
[36] Tchernycheva M *et al* 2007 *Nanotechnology* **18** 385306
[37] Songmuang R, Ben T, Daudin B, González D and Monroy E 2010 *Nanotechnology* **21** 295605
[38] Foxon C T, Novikov S V, Hall J L, Campion R P, Dherns D, Griffiths I and Khongsphetsak S 2009 *J. Cryst. Growth* **311** 3423
[39] Brault J, Gendry M, Grenet G, Hollinger G, Désières Y and Benyattou T 1999 *J. Cryst. Growth* **201/202** 1176
[40] Medhekar M V, Hegadekatte V and Shenoy V B 2008 *Phys. Rev. Lett.* **100** 106104
[41] Schulli T U *et al* 2009 *Phys. Rev. Lett.* **102** 025502
[42] Stringfellow G B 1972 *J. Appl. Phys.* **43** 3455
[43] Kawaguchi Y *et al* 1998 *J. Cryst. Growth* **189/190** 24
[44] Adelmann C, Simon J, Feuillet G, Pelekanos N T, Daudin B and Fischman G 2000 *Appl. Phys. Lett.* **76** 1570
[45] Graham D M, Soltani-Vala A, Dawson P, Godfrey M J, Smeeton T M, Barnard J S, Kappers M J, Humphreys C J and Thrush E J 2005 *J. Appl. Phys.* **97** 103508
[46] Chichibu S F *et al* 2006 *Nat. Mater.* **5** 810
[47] Bartel T P, Specht P, Ho J C and Kisielowski C 2007 *Phil. Mag.* **87** 1983
[48] Humphreys C J 2007 *Phil. Mag.* **87** 1971
[49] Bellaiche L, Mattila T, Wang L W, Wei S H and Zunger A 1999 *Appl. Phys. Lett.* **74** 1842